

## Thermal switching of the magnetization in an iron film on a magnetically active template MnAs/GaAs(001)

Maurizio Sacchi,<sup>1,2</sup> Massimiliano Marangolo,<sup>3</sup> Carlo Spezzani,<sup>4</sup> Romain Breitwieser,<sup>2</sup> Horia Popescu,<sup>1</sup> Renaud Dealaunay,<sup>2</sup> Benjamin Rache Salles,<sup>3</sup> Mahmoud Eddrief,<sup>3</sup> and Victor H. Etgens<sup>3</sup>

<sup>1</sup>Synchrotron SOLEIL, BP 48, 91192 Gif-sur-Yvette, France

<sup>2</sup>Laboratoire de Chimie Physique-Matière et Rayonnement, UPMC Paris 06, CNRS UMR 7614, 11 rue P. et M. Curie, 75005 Paris, France

<sup>3</sup>Institut des NanoSciences de Paris, UPMC Paris 06, CNRS UMR 7588, 140 rue de Lourmel, 75015 Paris, France

<sup>4</sup>Sincrotrone Trieste S.C.p.A., Area Science Park, S.S.14, Km 163.5, I-34012 Trieste, Italy

(Received 11 May 2010; published 2 June 2010)

We show that the magnetization direction of a thin Fe film can be fully reversed in a thermal cycle of a few degrees close to room temperature, without making use of an external magnetic field. This result is obtained by depositing the Fe film on MnAs/GaAs(001), which displays a temperature-controlled self-organized pattern of submicron-wide stripes, alternating ferromagnetic and nonmagnetic phases. The temperature-dependent dipolar fields generated by this magnetically active template can be used to control the magnetization of the Fe overlayer.

DOI: [10.1103/PhysRevB.81.220401](https://doi.org/10.1103/PhysRevB.81.220401)

PACS number(s): 75.70.-i

Means of orienting the magnetization of a thin film without making use of an external magnetic field are of considerable interest in fields related to the technology of sensors and of data storage devices. New methods for switching the magnetization aim at removing the need to generate cumbersome magnetic fields of sufficient strength at small length and time scales. Recently, electron currents,<sup>1</sup> polarized light,<sup>2</sup> or electric fields<sup>3</sup> have been invoked to alter and control the magnetization direction in ferromagnetic (FM) systems. Electric fields were also used to alter the magnetization state in hybrid ferromagnetic-piezoelectric systems.<sup>4</sup> We propose that the use of a nonhomogeneous magnetically active template (MAT) can provide alternative protocols for the local manipulation of the magnetic properties of a thin film. By MAT, we mean a system where intrinsic magnetic properties (such as Curie temperature, magnetization, or anisotropy) display a regular spatial modulation that can be controlled by tuning external parameters, e.g., strain or temperature. Our MAT is MnAs/GaAs(001), which presents a self-organized pattern of submicron-wide stripes,<sup>5</sup> alternating the FM hexagonal  $\alpha$ -MnAs phase with the nonferromagnetic (NM) orthorhombic  $\beta$ -MnAs phase [Fig. 1(a)]. In previous studies,<sup>6-8</sup> we found that the  $\alpha$ - $\beta$  modulation creates dipolar magnetic fields ( $H^D$ ) extending above the MnAs template.

In this Rapid Communication, we prove that the magnetization of the Fe overlayer can be fully reversed by tuning the MAT temperature, *without applying any external magnetic field*. We show also that this surprising property originates from the Fe lateral stripe patterning induced by the  $\alpha$ -MnAs dipolar field, i.e., the underlying  $\alpha/\beta$  MnAs magnetic modulation breaks the Fe thin films into independent magnetic entities presenting opposite magnetization.

MnAs has received renewed attention in the framework of the development of new devices, thanks to its good compatibility with standard semiconducting substrates<sup>9</sup> and to its high spin polarization.<sup>10</sup> By now, MnAs/GaAs(001) is a well understood metal/semiconductor system.<sup>11</sup> Over the phase-coexistence temperature region (roughly from 10–40 °C),

the period of the stripes is about five times the thickness of the MnAs layer, the step between  $\alpha$  and  $\beta$  stripes is 1–2 % of this thickness and the width of  $\beta$  stripes within a period increases continuously with temperature. Therefore, with MnAs/GaAs(001), we dispose of a MAT where nanometric steps separate microns long FM and NM stripes, whose width can be controlled by fine tuning the temperature around ambient.<sup>12</sup>

The sample was prepared at the Institut des NanoSciences de Paris by molecular-beam epitaxy. First, oxide desorption from the GaAs(001) substrate is carried out under As flux, then a thick GaAs layer is grown under As-rich conditions, with the substrate kept at  $T=560$  °C. The sample temperature is then reduced to 230 °C for depositing the 140-nm-thick MnAs template. Scanning tunnelling microscopy observations of the MAT show stripes with a period of  $\sim 700$  nm separated by steps of  $\sim 1.8$  nm, in agreement with predictions.<sup>5</sup> The 5-nm-thick Fe layer is deposited from a Knudsen cell on the template kept at a temperature of 150 °C, where MnAs is single phase ( $\gamma$  phase) and does not display any stripes. Finally, the sample is protected against contamination by 5 nm of Au.

We monitored the magnetic behavior of the sample by x-ray resonant magnetic scattering (XRMS) measurements at the Circular Polarization beamline of the synchrotron ELETTRA, using a reflectometer.<sup>13</sup> Data were collected in coplanar geometry, with the stripes of the MnAs template oriented normal to the scattering plane. At the photon energies used in our experiment (630–730 eV), the circular polarization rate of the x rays was  $\sim 70\%$  and the energy resolving power was set to 2000. The sample holder included a Peltier device for temperature control, as well as an electromagnet. An external magnetic field,  $H^{\text{ext}}$ , was applied along the intersection between the sample surface and the scattering plane, corresponding to the easy magnetization direction of  $\alpha$  MnAs. By using circularly polarized x rays and tuning the photon energy to the Mn  $2p$  ( $\sim 640$  eV) or to the Fe  $2p$  ( $\sim 707$  eV) absorption edges, the specular reflected intensity

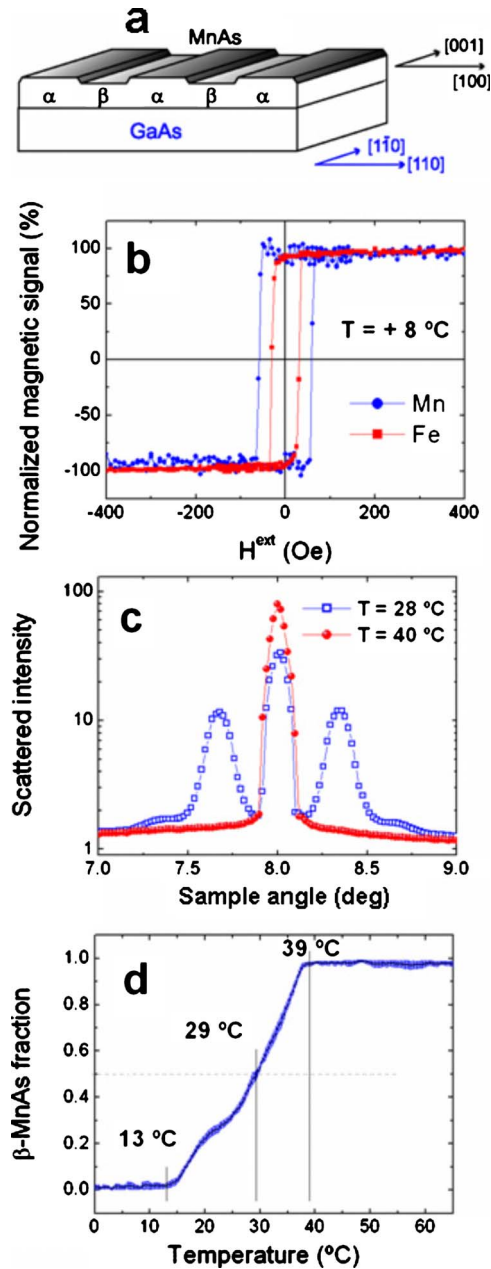


FIG. 1. (Color online) (a) Schematic view of MnAs thin films epitaxially on GaAs(001). (b) Low-temperature specular reflectivity ( $16^\circ$  scattering angle) as a function of  $H^{\text{ext}}$  at the Mn (●) and Fe (■)  $2p$  resonances. (c) Rocking curves ( $16^\circ$  scattering angle) at  $T=28^\circ\text{C}$  (phase coexistence) and  $T=40^\circ\text{C}$  ( $\beta$  phase). (d) Temperature-dependent fraction of  $\beta$  phase determined from rocking curve analysis. Vertical lines correspond to the onset ( $T=13^\circ\text{C}$ ), midpoint ( $T=29^\circ\text{C}$ ), and completion ( $T=39^\circ\text{C}$ ) of the  $\alpha$ - $\beta$  transformation.

is sensitive to the average magnetic moment carried by Mn atoms or by Fe atoms, respectively.<sup>14</sup> Element selectivity is essential for an independent analysis of MnAs and Fe magnetizations. In addition, the photon-in-photon-out character of the technique provides the measurement with a large probing depth and with imperviousness to magnetic fields. To complement our XRMS analysis, we performed also x-ray photoemission electron microscopy (X-PEEM) observations

on the SIM beamline of the SLS synchrotron source in Wigglingen (Switzerland). Tuning the circularly polarized photons at the Fe  $L_3$  resonance, X-PEEM provides element selective images of Fe magnetic domains with a spatial resolution better than 100 nm.

Figure 1 shows XRMS results that help describe the sample. Panel (b) shows the reflectivity at  $T=8^\circ\text{C}$  as a function of  $H^{\text{ext}}$ , measured at the Fe and Mn resonances. The two curves correspond to element selective hysteresis loops.<sup>14</sup> It turns out that the coupling between the two layers is weak since they display very different coercive fields of 58 Oe and 30 Oe for MnAs and Fe, respectively. Usually, the observation that two ferromagnetic layers are, at the same time, in contact and weakly coupled is ascribed to the formation of an interdiffused interface layer. In our previous work,<sup>6</sup> the formation of such a layer could not be detected explicitly. Panel (c) shows rocking scans (i.e., scattered intensity versus sample angle, at fixed detector angle), taken at two different temperatures. At  $T=40^\circ\text{C}$  (homogeneous  $\beta$  phase), one has only the specular peak while at  $T=28^\circ\text{C}$  ( $\alpha$ - $\beta$  coexistence), the spectrum displays Bragg diffraction peaks of first and second order originating from the regular pattern of the stripes. A quantitative analysis of the intensities of such peaks makes it possible to determine the average width of  $\alpha$  and  $\beta$  stripes,<sup>17</sup> leading to the estimate of the  $\beta$  fraction as a function of temperature given in Fig. 1(d). This curve is important since it provides all our measurements with a self-consistent temperature scale of the phase transition.

Figure 2(a) shows the main result of our experiment. After applying a magnetic pulse ( $H^{\text{ext}}=1$  kOe during 0.1 s) at  $T=8^\circ\text{C}$ , the sample temperature was cycled from 8 to  $18^\circ\text{C}$  (solid symbols) and back to  $8^\circ\text{C}$  (hollow symbols), without further application of an external field. Here, each point represents an asymmetry ratio (AR), i.e., the difference divided by the sum of two measurements performed with opposite orientations of the x-ray helicity with respect to the field direction of the initial magnetic pulse. At each resonance (squares for Mn and circles for Fe), the AR is proportional to the magnetic moment of the element.<sup>14</sup> As shown by the hysteresis loops of Fig. 1(b), the magnetic pulse at  $8^\circ\text{C}$  prepares the initial state of the thermal cycle of Fig. 2 with parallel Fe and MnAs magnetizations.

Figure 2(a) shows that the MnAs magnetization is barely affected when the temperature increases, in agreement with the fact that even at the highest temperature of  $18^\circ\text{C}$  less than 15% of MnAs is found in the  $\beta$  phase [Fig. 1(d)]. On the contrary, the Fe magnetization varies abruptly starting from  $T=13^\circ\text{C}$ , i.e., when the stripes set in [see Fig. 1(d)]. Over a few degrees, between  $T=13^\circ\text{C}$  and  $T=16^\circ\text{C}$ , the Fe magnetization switches sign, reaching an almost complete reversal. When returning to the initial temperature of  $+8^\circ\text{C}$ , the Fe/MnAs alignment is antiparallel (AP), i.e., opposite to the initial configuration, in spite of the fact that no external magnetic field has been applied throughout the entire cycle. We observed that the final Fe magnetization depends on the highest temperature  $T_{\text{max}}$  reached during the thermal cycle. A complete reversal of the Fe magnetization is obtained as long as  $\alpha$  MnAs retains the magnetization imposed by the initial magnetic pulse, prior to thermal cycling, i.e., up to  $T_{\text{max}} \approx 30^\circ\text{C}$ . For higher temperatures, the disordered distri-

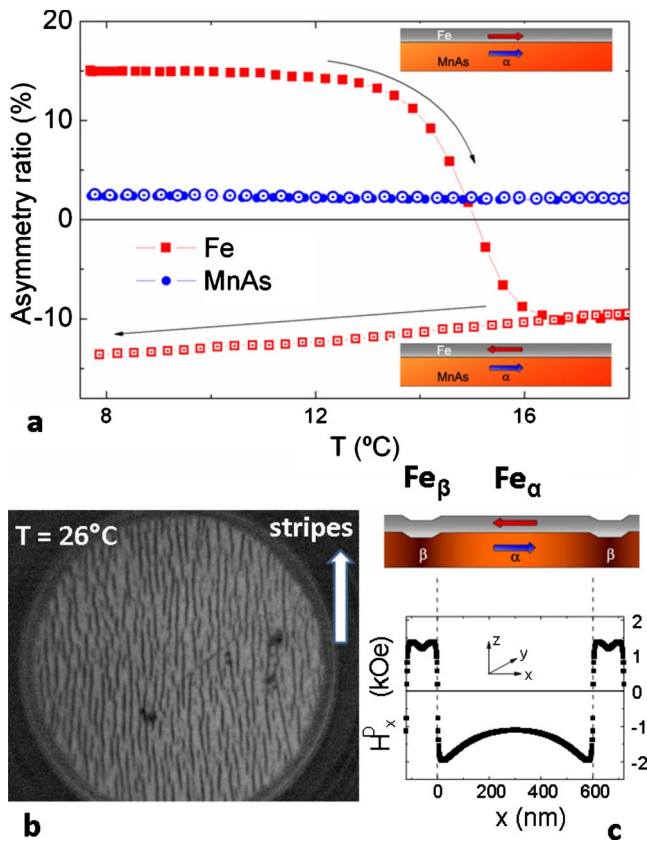


FIG. 2. (Color online) (a) Temperature dependence of the XRMS AR at the Fe ( $\square$ ,  $\blacksquare$ ) and Mn ( $\circ$ ,  $\bullet$ ) 2p resonances. The thermal cycle has a heating ( $\blacksquare$ ,  $\bullet$ ) and a cooling ( $\square$ ,  $\circ$ ) branch, between +8 and +18 °C. For each element, the AR is proportional to the magnetic moment projected along the direction normal to the stripes. (b) The Fe lateral stripe-patterned superstructure is clearly observed at 26 °C by X-PEEM measurements. (c)  $H_{Dx}$  component, calculated as a function of  $x$  at the center of the Fe overlayer (see text). Calculation parameters: constant magnetization of 640 emu/cm<sup>3</sup> with dimensions  $x=540$  nm (normal to the stripes),  $y=6$   $\mu$ m (along the stripes), and  $z=140$  nm (thickness). The  $H_{Dx}$  component was calculated (Ref. 16) as a function of  $x$  for  $y=3$   $\mu$ m and  $z=142.5$  nm, i.e., at the center of the 5-nm-thick Fe overlayer.

tribution of the MnAs domains<sup>15</sup> reduces drastically the efficiency of the MAT-driven switching process.

The Fe magnetization behavior shown in Fig. 2(a) can be understood by considering the intensity of the dipolar field  $H^D$  emanating from  $\alpha$ -MnAs stripes. In the schematic pictures of Fig. 2(c), we label the Fe sitting on top of  $\alpha$  and  $\beta$  stripes as Fe  $\alpha$  and Fe  $\beta$ , respectively. The magnetic poles of the finite-size  $\alpha$ -MnAs stripes generate a dipolar field outside of the MnAs itself, that we modeled assuming a bar-shaped MnAs magnet.<sup>16</sup> The result is shown in Fig. 2(c):  $H_x^D$  has opposite signs on top of  $\alpha$  and  $\beta$  stripes and its intensity ( $>1$  kOe) largely exceeds the 30 Oe coercive field of the Fe layer. Consequently, dipolar field could break the Fe magnetization in Fe  $\alpha$  and Fe  $\beta$  independent magnetic domains with opposite magnetizations, as suggested in Refs. 7 and 9. Since at  $T=+18$  °C, the  $\alpha$  phase dominates, the sign of the overall Fe magnetization is defined by the Fe  $\alpha$  one, which is

AP with respect to  $\alpha$  MnAs. During the cooling process, the Fe  $\alpha$  fraction expands, until a complete AP alignment between Fe and MnAs is attained.

The interpretation of the Fe film magnetization switching in terms of a very unusual lateral self-organization of Fe stripes with opposite magnetizations is supported by X-PEEM observations of Fe magnetic domains collected at the Fe  $L_3$  edges. As for XRMS data presented above, a magnetic field ( $H^{\text{ext}}=200$  Oe) was applied to the sample at 3 °C in order to prepare the initial state of the thermal cycle of Fig. 2 with parallel Fe and MnAs magnetizations. Then, *without further application of an external field*, the X-PEEM image of Fig. 2(b) was taken at 26 °C. The image shows clearly that the Fe layer is broken into magnetic domains (vertical stripes) separated by 180° domain walls confirming that an array of Fe  $\alpha$  (bright stripes) and Fe  $\beta$  (dark stripes) submicrometric magnetic domains is induced by the underlying MAT at room temperature. The magnetization of dark (bright) stripes is parallel (antiparallel) to the direction imposed by  $H^{\text{ext}}$ . Finally, returning at 8 °C produces a homogeneous bright image (not shown), i.e., the magnetization of Fe layer is opposite to the magnetic field that was applied at low temperature.

For further investigations, it is worth underlying that MnAs has a strong absorption band at around 3 eV,<sup>17</sup> suggesting that an efficient local heating of the MAT can be obtained using 400 nm radiation. Therefore, we anticipate that switching the magnetization of Fe on MnAs/GaAs(001) can be obtained locally by using focused laser radiation.

Our approach toward switching the magnetization of a ferromagnetic layer without applying an external magnetic field goes beyond the specific example illustrated here, the basic idea being that it is possible to modulate a template-generated dipolar field by controlling its temperature. An alternative to the epitaxial growth of MnAs films is to create a well-defined spatial modulation of  $T_C$  in a ferromagnetic substrate, for instance, by ion-beam irradiation<sup>18</sup> or by chemical doping.<sup>19</sup> The presence of two distinct  $T_C$  values ( $T_{Ca} < T_{Cb}$ ) plays the role of the phase-coexistence region for MnAs/GaAs(001). In this case too, we will have available a substrate that can be either magnetically homogeneous ( $T < T_{Ca}$ , no dipolar field) or inhomogeneous ( $T_{Ca} < T < T_{Cb}$ , dipolar field radiating at the level of the overlayer) as a function of temperature. In addition, the condition of weakly coupled adjacent ferromagnetic layers, that is, found for Fe on MnAs can be reproduced artificially for other systems by introducing a thin nonmagnetic spacer. Therefore, the design of magnetically active templates whose structural and magnetic properties are tailored to display specific and controlled temperature dependence around ambient temperature is a wide new field that may encompass different technical approaches.

We thank Sincrotrone Trieste and SLS for granting beamtime to our project. The Circular Polarization beamline staff provided technical assistance. We thank Armin Kleibert and F. Nolting for their support during XPEEM experiments at SLS and F. Vidal and J. Milano for useful discussions. This work received financial support from C’Nano-IdF (project TRIPEPS).

- <sup>1</sup>M. Yamanouchi, D. Chiba, F. Matsukura, and H. Ohno, *Nature (London)* **428**, 539 (2004).
- <sup>2</sup>A. V. Kimel, A. Kirilyuk, P. A. Usachev, R. V. Pisarev, A. M. Balbashov, and Th. Rasing, *Nature (London)* **435**, 655 (2005).
- <sup>3</sup>D. Chiba, M. Sawicki, Y. Nishitani, Y. Nakatani, F. Matsukura, and H. Ohno, *Nature (London)* **455**, 515 (2008); M. Saito, K. Ishikawa, S. Konno, K. Taniguchi, and T. Arima, *Nature Mater.* **8**, 634 (2009).
- <sup>4</sup>S. Sahoo, S. Polisetty, C.-G. Duan, S. S. Jaswal, E. Y. Tsymbal, and C. Binek, *Phys. Rev. B* **76**, 092108 (2007).
- <sup>5</sup>V. M. Kaganer, B. Jenichen, F. Schippan, W. Braun, L. Däweritz, and K. H. Ploog, *Phys. Rev. B* **66**, 045305 (2002).
- <sup>6</sup>M. Sacchi, M. Marangolo, C. Spezzani, L. Coelho, R. Breitwieser, J. Milano, and V. H. Etgens, *Phys. Rev. B* **77**, 165317 (2008).
- <sup>7</sup>R. Breitwieser, M. Marangolo, J. Lüning, N. Jaouen, L. Joly, M. Eddrief, V. H. Etgens, and M. Sacchi, *Appl. Phys. Lett.* **93**, 122508 (2008).
- <sup>8</sup>S. Tacchi, M. Madami, G. Carlotti, G. Gubbiotti, M. Marangolo, J. Milano, R. Breitwieser, V. H. Etgens, R. L. Stamps, and M. G. Pini, *Phys. Rev. B* **80**, 155427 (2009).
- <sup>9</sup>M. Tanaka, J. P. Harbison, M. C. Park, Y. S. Park, T. Shin, and G. M. Rothberg, *J. Appl. Phys.* **76**, 6278 (1994).
- <sup>10</sup>V. Garcia, H. Jaffrès, J.-M. George, M. Marangolo, M. Eddrief, and V. H. Etgens, *Phys. Rev. Lett.* **97**, 246802 (2006).
- <sup>11</sup>L. Däweritz, C. Herrmann, J. Mohanty, T. Hesjedal, K. H. Ploog, E. Bauer, A. Locatelli, S. Cherifi, R. Belkhou, A. Pavlovska, and S. Heun, *J. Vac. Sci. Technol. B* **23**, 1759 (2005).
- <sup>12</sup>R. Breitwieser, F. Vidal, I. L. Graff, M. Marangolo, M. Eddrief, J.-C. Boulliard, and V. H. Etgens, *Phys. Rev. B* **80**, 045403 (2009).
- <sup>13</sup>M. Sacchi, C. Spezzani, P. Torelli, A. Avila, R. Delaunay, and C. F. Hague, *Rev. Sci. Instrum.* **74**, 2791 (2003).
- <sup>14</sup>M. Sacchi, A. Mirone, C. F. Hague, J. M. Mariot, L. Pasquali, P. Isberg, E. M. Gullikson, and J. H. Underwood, *Phys. Rev. B* **60**, R12569 (1999).
- <sup>15</sup>L. N. Coelho, B. R. A. Neves, R. Magalhães-Paniago, F. C. Vicentin, H. Westfahl, Jr., R. M. Fernandes, F. Iikawa, L. Däweritz, C. Spezzani, and M. Sacchi, *J. Appl. Phys.* **100**, 083906 (2006); R. Engel-Herbert and T. Hesjedal, *Phys. Rev. B* **78**, 235309 (2008).
- <sup>16</sup>J. Norpoth, S. Dreyer, and C. Joss, *J. Phys. D* **41**, 025001 (2008).
- <sup>17</sup>B. Gallas, J. Rivory, H. Arwin, F. Vidal, and M. Stchakovsky, *Phys. Status Solidi A* **205**, 859 (2008).
- <sup>18</sup> $T_C$  control by ion irradiation has been observed in several transition-metal alloys, such as Mn-Ni, Fe-Ni, and Fe-Pt. Similar results have been reported also for the magnetic semiconductor (GaMn)As: H. Kato, K. Hamaya, Y. Kitamoto, T. Taniyama, and H. Munekata, *J. Appl. Phys.* **97**, 10D302 (2005).
- <sup>19</sup>L. Thevenard, L. Largeau, O. Mauguin, A. Lemaître, and B. Theys, *Appl. Phys. Lett.* **87**, 182506 (2005); K. Khazen, H. J. von Bardeleben, J. L. Cantin, L. Thevenard, L. Largeau, O. Mauguin, and A. Lemaître, *Phys. Rev. B* **77**, 165204 (2008).